Book: Geotechnical Earthquake Engineering and Soil Dynamics V: Numerical Modeling and Soil Structure Interaction
Year: 2018

Evaluation of the ISA-Hypoplasticity Constitutive Model for the LEAP-2017 Project

William Fuentes, Ph.D.[1]; Vicente Mercado, Ph.D.[2]; and Carlos Lascarro[3]

[1]Univ. del Norte, Dept. of Civil and Environmental Engineering, Barranquilla, Colombia. E-mail: fuentesw@uninorte.edu.co
[2]Univ. del Norte, Dept. of Civil and Environmental Engineering, Barranquilla, Colombia. E-mail: vmercado@uninorte.edu.co
[3]Univ. del Norte, Dept. of Civil and Environmental Engineering, Barranquilla, Colombia. E-mail: cjlascarro@uninorte.edu.co

ABSTRACT

In this work the capabilities of the ISA-hypoplasticity model for the simulation of a sandy material are carefully analyzed. The ISA-hypoplasticity model is based on the hypoplastic model by von Wolfferdorff (1996), extended by the intergranular strain anisotropy (ISA) concept by Fuentes and Triantafyllidis (2015). The model is able to simulate monotonic and cyclic loading, and has been recently modified to consider the cyclic mobility effect. Within this work, a calibration procedure has been conducted to determine the material parameters of Ottawa F65 sand and a set of experiments showing monotonic and cyclic loading has been simulated. This work is embedded within the liquefaction experiments and analysis projects (LEAP), which seeks to assess and improve the current numerical tools for prediction and evaluation of soil liquefaction phenomena.

INTRODUCTION

Accurate prediction of the behavior of soil deposits subjected to liquefaction is essential in order to guarantee the safety of civil infrastructure. There is still a considerable degree of uncertainty in the available numerical methodologies that are currently being used. Within this context, a validation campaign, the Liquefaction Experiment and Analysis Project (LEAP), has been launched in order to assess the capabilities of existing numerical/constitutive models for liquefaction analysis by using laboratory experiments and centrifuge tests (Manzari, et al., 2014).

The current work is embedded within the LEAP-2017 project, and it seeks to analyze the capabilities of the ISA-Hypoplasticity model for the simulation of a sandy material. This constitutive model is based on the constitutive model the hypoplastic model by von Wolfferdorff (1996) rewritten according to the Intergranular Strain Anisotropy plasticity (ISA-plasticity) constitutive platform. The intergranular strain concept proposed by Niemunis and Herle (1997) is incorporated into the model, but following the recent formulation of Fuentes and Triantafyllidis (2015).

A numerical implementation for finite element codes has been performed in FORTRAN following the syntax for the subroutine UMAT from the program ABAQUS. The simulations were made using the open-source software Incremental Driver created by Niemunis (2008) but modified by the authors of this work to improve the code for cyclic loading. The algorithm is semi-explicit, meaning that most equations were solved explicitly except by a few equations concerning the intergranular strain.

BRIEF DESCRIPTION OF ISA PLASTICITY

The formulation of the ISA-plasticity is hereby outlined. Details and additional information

of the model are found in (Fuentes, 2014) and (Fuentes & Triantafyllidis, 2015). This theory uses the same concept of intergranular strain proposed by Niemunis and Herle (1997) but reformulates previous definitions by incorporating an elastic locus which allows for "memory" effects during cyclic loading. This locus is obtained for strain amplitudes smaller than $\| \Delta\epsilon \| < R$, where R corresponds to the elastic strain amplitude. A good approximation that fits well with experimental observations with sand samples, and which also does not generate numerical difficulties in the integration of the model corresponds to $R \approx 10^{-4}$.

The intergranular strain is a strain-type state variable denoted by $\boldsymbol{h}$ that has its own evolution equation. Under elastic conditions, the intergranular strain evolves identically with the strain ϵ:

$$\dot{\boldsymbol{h}} = \epsilon \,(\text{elastic conditions}) \tag{1}$$

This allows for the definition of a yield surface having a spherical shape within the principal space of the intergranular strain to guarantee an elastic locus with a specific strain amplitude $\| \Delta\epsilon \| = R$:

$$F_H = \left\| \boldsymbol{h} - \boldsymbol{c} \right\| - \frac{R}{2} \,(\text{yield surface}) \tag{2}$$

whereby R is a material parameter representing the strain amplitude and $\boldsymbol{c}$ is a tensor representing the center of the yield surface and therefore called the back-intergranular strain.

When the amplitude of the deformation is greater than R, the yield surface is expected to be equal to $F_H = 0$. Under this condition, the evolution equation of intergranular deformation is:

$$\dot{\boldsymbol{h}} = \epsilon - \lambda_H \, \mathbf{N} \tag{3}$$

whereby λ_H is the consistency parameter (or plastic multiplier) and $\mathbf{N}$ is the flow rule which reads:

$$\mathbf{N} = \frac{\partial F_H}{\partial \boldsymbol{h}} = \frac{\boldsymbol{h} - \boldsymbol{c}}{(R/2)} \tag{4}$$

The consistency parameter vanishes under elastic conditions $\lambda_H = 0$ and takes its maximum value $\lambda_H = \epsilon$ at the bounding surface of the intergranular strain. The shape of the bounding surface is also spherical but with fixed center at $\boldsymbol{h}$ =0 and diameter equal to $2R$, i.e. it presents twice the size of the yield surface. The bounding surface function F_{Hb} reads:

$$F_{Hb} = \left\| \boldsymbol{h} \right\| - R\left(\textit{bounding surface} \right) \tag{5}$$

The hardening rule for the back-intergranular strain $\boldsymbol{c}$ uses similar ideas to the bounding surface plasticity (Dafalias, 1986). For this purpose, we project an image tensor of $\boldsymbol{c_b}$ at the bounding surface with the following mapping rule

$$\boldsymbol{c_b} = (R/2)\vec{\epsilon}(\textit{image of in the bounding surface}) \tag{6}$$

where $\vec{\epsilon}$ represents the direction of the strain rate. The hardening function $\bar{\boldsymbol{c}} = \dot{\boldsymbol{c}} / \dot{\lambda}$ reads:

$$\bar{\boldsymbol{c}} = \frac{\beta_h \left(\boldsymbol{c}_b - \boldsymbol{c} \right)}{R} \text{ with } \dot{\boldsymbol{c}} = \dot{\lambda}_H \bar{\boldsymbol{c}} \left(\textit{hardening equation} \right) \tag{7}$$

where β_h is an additional parameter to control the rate of $\boldsymbol{c}$. Notice that if $\boldsymbol{c_b} = \boldsymbol{c}$ then the rate

$\bar{\boldsymbol{c}} = 0$ vanishes. Hence for very large strains, the model gives $\boldsymbol{h}_b = \boldsymbol{h}$, $\boldsymbol{c}_b = \boldsymbol{c}$ (see Figure 1). The expression for the consistency parameter is deduced by simple plasticity relations from the consistency equation $F_H = 0$ and reads:

$$\dot{\lambda}_H = \frac{\mathbf{N} : \dot{\epsilon}}{1 - \frac{\partial F_H}{\partial \boldsymbol{c}} : \bar{\boldsymbol{c}}} \left(\textit{consistency parameter} \right) \tag{8}$$

whereby the operator $\langle x \rangle = x$ when $x > 0$ and $\langle x \rangle = 0$ if $x \leq 0$. The equations 2-8 conform the model of the intergranular strain alone. This model evolves in parallel with the mechanical model but independently because it does not depend on the stress tensor $\boldsymbol{\sigma}$. The ISA-plasticity introduces some additional scalar factors to use the information provided by the intergranular strain model. These scalar factors depend on the projection of the intergranular strain $\boldsymbol{h}$ at the bounding surface using the flow rule $\mathbf{N}$ as the mapping tensor:

$$\mathbf{h}_b = R\mathbf{N} \ (\textit{image of in the bounding surface}) \tag{9}$$

where $\mathbf{h}_b$ is the projected tensor. Aided by tensor $\mathbf{h}_b$, one may detect some recent movements in the loading history. For example, if $\| \mathbf{h}_b - \mathbf{h} \| = 0$, it means that the current intergranular strain lies at its bounding condition. According to the model, this condition is only reached under large strain amplitudes and is therefore called "mobilized states". On the other hand, greater values of $\| \mathbf{h}_b - \mathbf{h} \| > 0$ represent a reversal loading which has been recently performed. Hence, the model proposes the function ρ as:

$$\rho = 1 - \frac{|\,|\mathbf{h}_b - \mathbf{h}|\,|}{2R} \left(\textit{factor of intergranular strain} \right) \tag{10}$$

In this manner, $\rho = 0$ implies reversal loading while $\rho = 1$ implies "mobilized states". In the next section, the mechanical model will be briefly described.

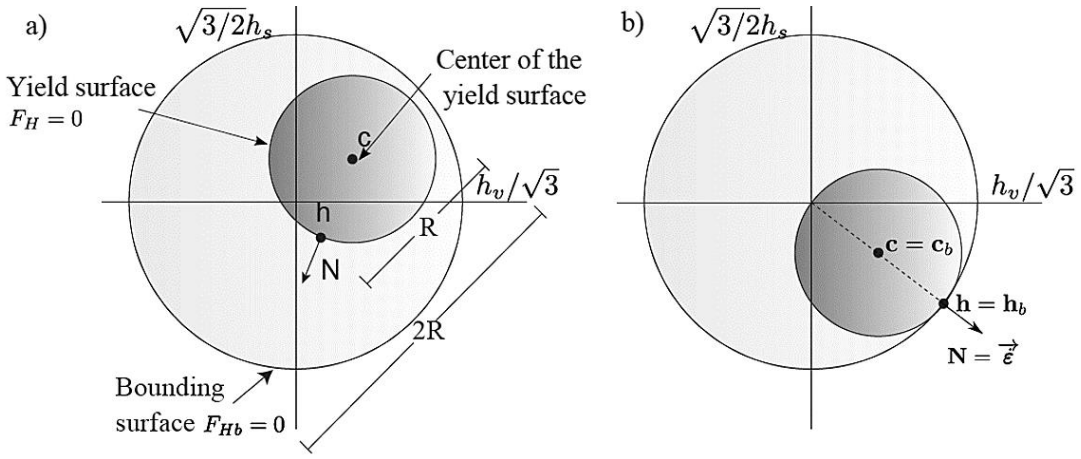

Figure 1. Schematic of the yield surface and the bounding surface within the intergranular strain principal space. (a) Geometry. (b) Example of the bounding condition (F_{Hb}=0).

DESCRIPTION OF THE MECHANICAL MODEL

The mechanical model relates the stress rate $\boldsymbol{\sigma}$ with the strain rate $\dot{\boldsymbol{\varepsilon}}$ through a constitutive equation. For this theory, the constitutive equation presents the following general form:

$$\dot{\boldsymbol{\sigma}} = m\bar{\mathbf{E}} : \left(\dot{\boldsymbol{\varepsilon}} - y_h \dot{\bar{\boldsymbol{\varepsilon}}}^{p} \right) \left(general\ equation \right) \tag{11}$$

where m and y_h are scalar functions, $\bar{\mathbf{E}}$ and $\dot{\bar{\boldsymbol{\varepsilon}}}^{p}$ are called "mobilized" stiffness tensor and "mobilized" plastic strain rate respectively. Tensors $\bar{\mathbf{E}}$ and $\dot{\bar{\boldsymbol{\varepsilon}}}^{p}$ can be adjusted to existing relations of hypoplastic models, e.g. (Herle & Kolymbas, 2004; Masin, 2005; von Wolffersdorff, 1996). Actually, when the intergranular strain lies under mobilized states, the scalar functions render $m = 1$ and $y_h = 1$ and the model yields to:

$$\dot{\boldsymbol{\sigma}} = \bar{\mathbf{E}} : (\dot{\boldsymbol{\varepsilon}} - \dot{\bar{\boldsymbol{\varepsilon}}}^{p}) \left(for\ mobilized\ state \right) \tag{12}$$

This mathematical form is actually not recognized as a formal hypoplastic model (Kolymbas, 2000). Users of the Hypoplasticity family are rather familiar with the equation:

$$\dot{\boldsymbol{\sigma}} = \mathbf{L}^{hyp} : \dot{\varepsilon} + \mathbf{N}^{hyp} \left| \left| \dot{\boldsymbol{\varepsilon}} \right| \right| \left(conventional\ hypoplastic\ model \right) \tag{13}$$

whereby $\mathbf{L}^{hyp}$ is the "linear" stiffness and $\mathbf{N}^{hyp}$ is the "non-linear" stiffness (Herle & Kolymbas, 2004; Masin, 2005; von Wolffersdorff, 1996; Wu & Niemunis, 1996). Existing relations for tensors $\mathbf{L}^{hyp}$ and $\mathbf{N}^{hyp}$ can be adopted for the present theory when setting the following equivalencies:

$$\mathbf{L}^{hyp} = \bar{\mathbf{E}} \left(linear\ stiffness,\ 4^{th} order\ tensor \right) \tag{14}$$

$$\mathbf{N}^{hyp} = -(\mathbf{E} : \dot{\bar{\boldsymbol{\varepsilon}}}^{p}) / \left| \left| \dot{\boldsymbol{\varepsilon}} \right| \right| \left(non-linear\ stiffness,\ 2^{nd} order\ tensor \right) \tag{15}$$

We have selected the hypoplastic model by von Wolffersdorff (1996) for the present work considering that our interest is the simulation of sand.

The scalar function y_h is a factor which ranges between $0 \le y_h \le 1$ and aims to reduce the plastic strain rate after reversal loading. The function y_h reads:

$$y_h = \rho^{\chi} \mathbf{N} : \vec{\varepsilon} \left(factor\ for\ decrease\ in\ the\ rate\ of\ plastic\ deformations \right) \tag{16}$$

where χ is an exponent which can be set as a material constant (Fuentes & Triantafyllidis, 2015), or improved to account for the effect of repetitive loading within the plastic accumulation rate (Poblete, Fuentes, & Triantafyllidis, 2016). The function m aims to increase the stiffness upon reversal loading. This function reads:

$$m = m_R + (1 - m_R) y_h \left(factor\ for\ increase\ of\ stiffness \right) \tag{17}$$

where m_R is a material constant to increase the stiffness under elastic conditions.

The recent modification by Poblete et al. (2016) included the modification of exponent χ to improve the simulations under repetitive loading. In order to detect whether a few or a number of subsequent cycles have been performed, they proposed an additional state variable ε_{acc} with the following evolution law:

$$\dot{\varepsilon}_{acc} = \frac{C_a}{R} (1 - y_h - \varepsilon_{acc}) \left| \left| \dot{\varepsilon} \right| \right| \left(state\ variable\ for\ detection\ of\ repetitive\ cycles \right) \tag{18}$$

whereby C_a is a material parameter controlling the rate of $\dot{\varepsilon}_{acc}$ (Poblete, Fuentes, & Triantafyllidis, 2016). Notice that if one performs subsequent cycles, the function y_h reduces its value $y_h \to 0$ and the state variable ε_{acc} starts to increase. Hence, one can use this information

to reduce the plastic strain rate upon subsequent cycles which are now detected with the condition $\varepsilon_{acc} > 0$. To achieve this, the exponent χ is reduced according to the relation:

$$\chi = \chi_0 + \varepsilon_{acc}(\chi_{\max} - \chi_0)\left(\textit{modification to capture effects of repetitive cycles}\right) \tag{19}$$

whereby χ_0 and $\chi_{\max}$ are material constants. The first should be adjusted for small number of cycles $N < 3$ and the other for large number of cycles (e.g. $N > 15$).

The continuum (explicit) stiffness $\mathbf{M} = (\partial\dot{\boldsymbol{\sigma}} / \partial\dot{\boldsymbol{\varepsilon}})$ of the model can be deduced after derivation of the constitutive equation such that it reduces to:

$$\dot{\boldsymbol{\sigma}} = \mathbf{M} : \dot{\boldsymbol{\varepsilon}}\left(\textit{equation with con continuum stiffness tensor}\right) \tag{20}$$

whereby the continuum stiffness $\mathbf{M}$ reads:

$$\mathbf{M} = \begin{cases} \left[m_R + (1 - m_R)\, y_h\right]\left(\boldsymbol{L}^{hyp} + \rho^{\chi}\boldsymbol{N}^{hyp} \otimes \boldsymbol{N}\right) \textit{ for } F_h \geq 0 \\ m_R \mathbf{L}^{hyp} \textit{ for } F_h < 0 \end{cases} \tag{21}$$

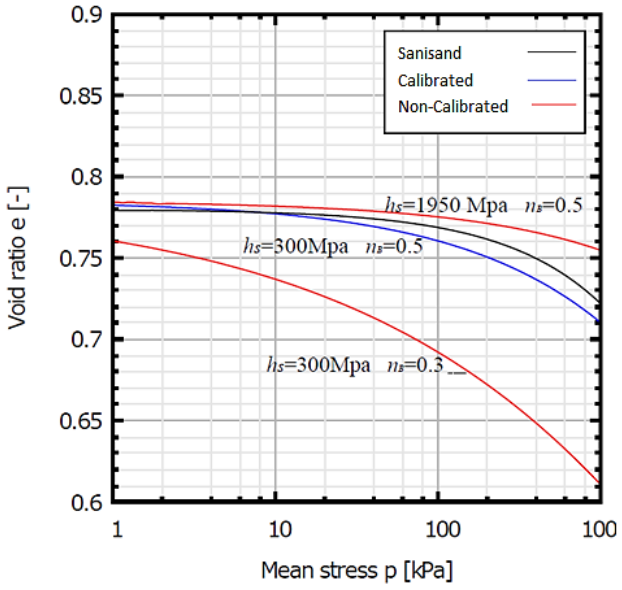

Figure 2. Calibration of h_s and n_B using Oedometric test simulation, data from (Parra, 2016).

CALIBRATION METHOD

A short guide for the determination of the parameters is provided.

- The critical state friction angle φ_c can be adjusted with points of a triaxial compression test after a vertical strain of ε_1 >25%. The critical state slope within the *p*-*q* space can be calibrated with the relation $q / p = 6 \sin\varphi_c / (3 - \sin\varphi_c)$ for these points.
- The maximum void ratio at *p*=0 denoted with $e_i o$ can be obtained through the standardized minimum density test (ASTM D4254-14).
- The exponent n_B can be adjusted to match the elastic stiffness dependence with the mean pressure $G \backsim p^{1-n_B}$ through the results of resonant column test for different

confining pressures. If the experiments are scarce, some values from the literature can be adopted, e.g. n_B =0.5.

- The granular hardness h_s can be adjusted to simulate the oedometric compression stiffness under very loose states $e \approx e_i$ where $e_i = e_i(p)$ is the maximum void ratio curve (see Figure 2).
- The critical state void ratio at *p*=0 denoted with $e_c o$ can be adjusted from points lying at the critical state (ε_1 >25% with triaxial compression) in the *e-p* space with very low pressure *p* <20 kPa. When data is scarce, one may adopt the approximation $e_c o \approx 0.9 e_i o$.
- The dilatancy exponent α is calibrated with the behavior of medium-dense and dense samples sheared through drained triaxial compression. This parameter controls the dilatancy rate of the volumetric strains after reaching the phase of transformation line.
- The barotropy exponent β is adjusted to dense samples compressed under oedometric conditions.
- The parameter *R* defines the size of the elastic locus in terms of strain increments. For the secant shear stiffness G^{sec}, this can be interpreted as the strain range at which no degradation occurs. Many experiments point a value of approximately $\| \Delta\epsilon \| \approx 10^{-5}$ for sands, but a small value of this parameter may lead to numerical difficulties when dealing with finite element simulations. Hence, a value of $\| \Delta\epsilon \| > 5 \times 10^{-5}$ is recommended.
- The parameter β_h controls the needed strain increment to eliminate the influence of the intergranular strain effect in the model. In other words, it controls the size of the strain amplitude at which no "small strain effects" is simulated by the model. The equation relating this strain amplitude with the parameter β_h reads:

$$\beta_h = \frac{\sqrt{6} R \left(\log(4) - 2\log(1 - r_h) \right)}{6 \Delta\varepsilon_s - \sqrt{6} R (3 + r_h)} \tag{22}$$

where $\Delta\varepsilon_s$ is the deviatoric strain amplitude and $r_h \approx 0.99$ is a factor which defines how close is tensor $\boldsymbol{c}$ to its bounding condition $r_h = \boldsymbol{c} / \boldsymbol{c_b}$.

The parameter χ controls the degradation curve shape of the secant shear modulus G^{sec}. Its calibration can be performed simulating some cycles of triaxial test.

The parameter C_a controls how fast the plastic accumulation rate reduces upon the cycles. It can be adjusted with a cyclic undrained triaxial test with the behavior of the accumulated pore pressure p_w^{acc} vs. the number of cycles *N*. The first portion of this curve, with approximately *N* <10, can be adjusted through parameter C_a by trial and error.

The parameter χ_{max} controls the accumulation rate when the number of consecutive cycles is large, of about *N* >10. It can be adjusted with a cyclic undrained triaxial test with the behavior of the accumulated pore pressure p_w^{acc} vs. the number of cycles *N*. An increasing number of χ_{max} would return a lower value of *N* to reach failure at the critical state line. It can be adjusted by trial and error after fixing C_a.

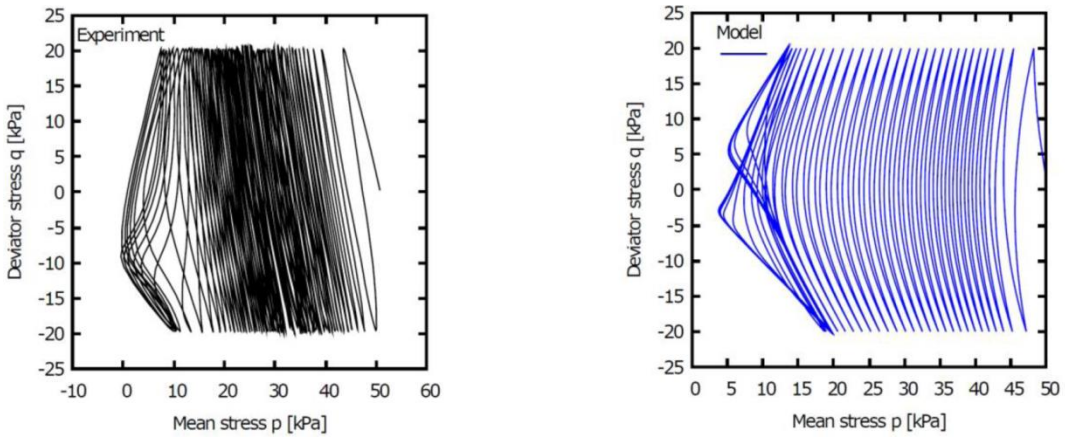

Figure 3. Undrained triaxial test under cyclic loading. Deviator stress amplitude of q^{amp}=20kPa, p_0= 50 kPa. Experiment using Ottawa F65 sand.

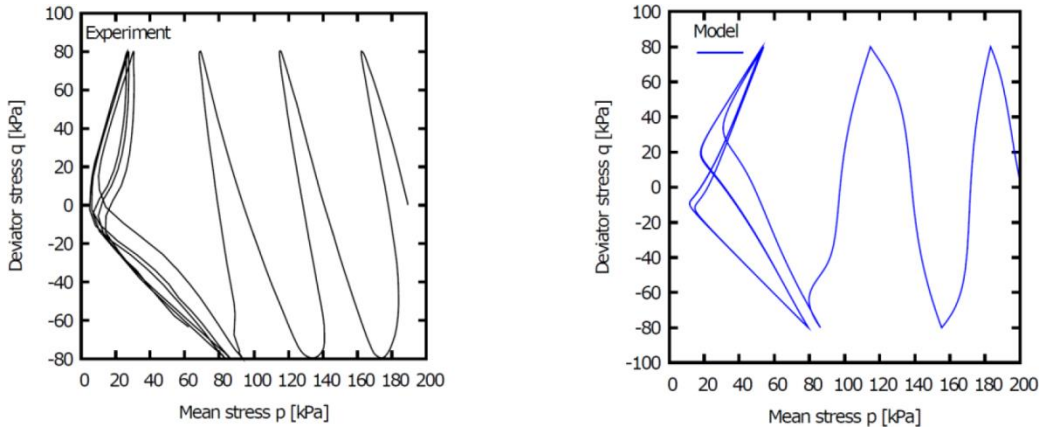

Figure 4. Undrained triaxial test under cyclic loading. Deviator stress amplitude of q^{amp}=80kPa, p_0= 200 kPa. Experiment using Ottawa F65 sand.

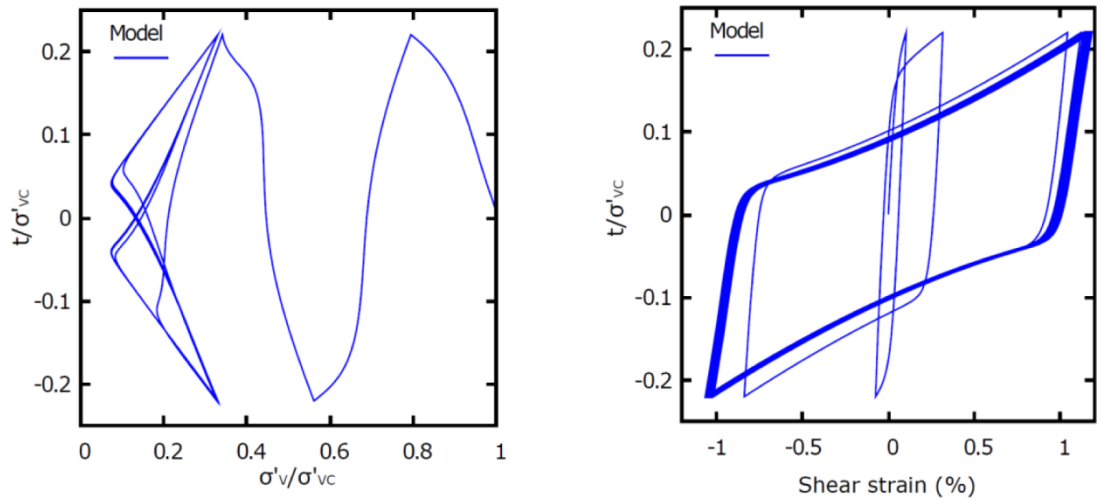

Figure 5. Simulated response of cyclic undrained simple shear test for Ottawa sand $\sigma_{vc}^{'} = 100$ kPa sheared up to γ=1%

Table 1 Model parameters obtained from the calibration process.

	Description	Unity	Value
Hypoplasticity (von Wolfferdorff)			
φ_c	Critical friction angle	[^{0}]	32^o
h_s	Granular hardness	[MPa]	300
n_B	Barotropy exponent	[-]	0.5
$e_i o$	Maximum void ratio	[-]	0.850
$e_c o$	Critical void ratio	[-]	0.785
$e_d o$	Minimal void ratio	[-]	0.500
α	Dilatancy exponent	[-]	0.1
β	Density exponent	[-]	2.0
ISA Model			
m_R	Stiffness factor	[-]	3.5
R	IS yield surface radius	[-]	1.0×10^{-4}
β_h	IS hardening parameter	[-]	0.5
χ_0	Minimum value of χ	[-]	4
Extension by Poblete, Fuentes, and Triantafyllidis (2016):			
C_a	Control for rate of e^{acc}	[-]	0.15
χ_{max}	Maximum value of χ	[-]	15

SIMULATION RESULTS

Procedures in the previous section were followed to calibrate model parameters in order to replicate the behavior of Ottawa F65 sand used for the LEAP- 2017 project. Model parameters associated to von Wolfferdorff´s hypoplasticity (von Wolffersdorff, 1996) are obtained based on monotonic triaxials and oedometric test. Maximum and minimum void ratios were obtained based on standardized laboratory tests. Parameters associated to the ISA-plasticity are calibrated based on cyclic triaxial tests. Model parameters obtained from the calibration process are summarized in Table 1.

Figure 3, for instance, shows the simulation of a cyclic undrained triaxial test along with laboratory results. For this test the sample was isotropically consolidated to a mean stress of p = 50 kPa and loaded under triaxial conditions. Figure 4, on the other hand, also show laboratory test results, along with numerical simulations of another cyclic triaxial performed using an initial mean confining stress of p = 200 kPa. The depicted experiments correspond to a test density e_0 = 0.542. These simulations consider an element test condition, meaning that homogeneous fields of stress and strain are assumed. Figures 3 and 4 evidence the capabilities of the calibrated model to replicate the contractive behavior of the tested sand, and the subsequent observed dilation.

Results for a cyclic undrained simple shear test are depicted in Figure 5, for illustrative

purposes. This figure shows simulation results for a test having an initial effective vertical stress $\sigma'_{vc} = 100$ kPa . Normalized shear stress vs. normalized effective vertical stress, and shear stress – strain behavior are depicted. These results also exhibit a modulus reduction and a reduction of the confining stress followed by a dilative response, as expected for the simulated sand.

CONCLUSIONS

An ISA-plasticity based model has been used to simulate the response of Ottawa F65 sand. For large strain amplitudes $\|\delta\varepsilon\| > 10^{-2}$, the model delivers the hypoplastic relation by (von Wolffersdorff, 1996). The extension by (Fuentes & Triantafyllidis, 2015) was herein considered to simulate the reduction of the plastic accumulation for increasing number of subsequent cycles. Numerical simulations were performed using element tests with cyclic loading yielding satisfactory results. The model was able to approximately capture the number of cycles leading to the liquefaction of the material. The model is currently being improved in order to better capture the cyclic mobility effect and the post-liquefaction behavior.

REFERENCES

Dafalias, Y. F. (1986). Bounding surface plasticity. I: Mathematical foundation and hypoplasticity. *J. Engrg. Mech, 112*(9), 966-987.

Fuentes, W., & Triantafyllidis, T. (2015). ISA model: A constitutive model for soils with yield surface in the intergranular strain space. *Int. J. Numer. Anal. Meth. Geomech, 39*(11), 1235-1254.

Herle, I., & Kolymbas, D. (2004). Hypoplasticity for soils with low friction angles. *Computers and Geotechnics, 31*(5), 365-373.

Kolymbas, D. (2000). *Introduction to Hypoplasticity.* (1st ed.). Rotterdam, Netherlands: A.A. Balkema.

Manzari, M., Kutter, B., Zeghal, M., Iai, S., Tobita, T., Madabhushi, S., Haigh, S., Mejia, L., Gutierrez, D., Armstrong, R.J., & Sharp, M. (2014). LEAP projects: concept and challenges. *Proceedings, 4th International Conference on Geotechnical Engineering for Disaster Mitigation and Rehabilitation,* (pp. 109-116).

Masin, D. (2005). A hypoplastic constitutive model for clays. *Int. J. Numer. Anal. Meth. Geomech, 29*(4), 311-336.

Niemunis, A. (2008). *Incremental Driver. User's Manual.* University of Karlsruhe, Germany.

Niemunis, A., & Herle, I. (1997). Hypoplastic model for cohesionless soils with elastic strain range. *Mechanic of cohesive-frictional materials, 2*(4), 279-299.

Parra, A. (2016). Ottawa f-65 sand characterization (Ph.D. thesis). University of California, Davis.

Poblete, M., Fuentes, W., & Triantafyllidis, T. (2016). On the simulation of multidimensional cyclic loading with intergranular strain. *Acta Geotechnica, 11*(6), 1263-1283.

von Wolffersdorff, P. (1996). A hypoplastic relation for granular materials with a predeffined limit state surface. *Mechanics of cohesive-frictional materials, 1*(3), 251-271.

Wu, W., & Niemunis, A. (1996). Failure criterion,flow rule and dissipation function derived from hypoplasticity. *Mechanics of Cohesive-Frictional Materials, 1*(2), 145-165.